ALKALINE OXIDE CONVERSION COATINGS FOR ALUMINUM ALLOYS*

R.G. Buchheit
Sandia National Laboratories
Albuquerque, New Mexico 87185

ABSTRACT

Three related conversion coating methods are described that are based on film formation which occurs when aluminum alloys are exposed to alkaline Li salt solutions. Representative examples of the processing methods, resulting coating structure, composition and morphology are presented. The corrosion resistance of these coatings to aerated 0.5 M NaCl solution has been evaluated as a function of total processing time using electrochemical impedance spectroscopy (EIS). This evaluation shows that excellent corrosion resistance can be uniformly achieved using no more than 20 minutes of process time for 6061-T6. Using current methods a minimum of 80 minutes of process time is required to get marginally acceptable corrosion resistance for 2024-T3. Longer processing times are required to achieve uniformly good corrosion resistance.

Keywords: hydrotalcite, conversion coating, corrosion resistance, aluminum alloys, electrochemical impedance spectroscopy.

**This work was performed at Sandia National Laboratories under contract DE-AC04-94AL85000.*

INTRODUCTION

Commercial chromate/chromic acid conversion coating processes were first introduced in 1945[1] as a method to improve the corrosion resistance and paint adhesion of many metal alloy systems. These processes are now regarded as technologically mature. These processes are trusted and used widely in automotive, aerospace, architectural and consumer durables applications.

In 1993, approximately 45,000 tons of Cr were used in metal finishing operations[2]. The total value of Cr-based finishing chemicals used was $250 million. These chemicals are critical to providing corrosion protection for fabricated aluminum components whose 1993 annual value was estimated to exceed $22 billion[3].

Chromate and chromic acid contain chromium in its hexavalent oxidation state, Cr^{6+}. Hexavalent chromium is a potent human carcinogen and is identified as a hazardous substance in federal legislation including the Clean Water Act, Clean Air Act and the Comprehensive Environmental Recovery Compensation and Liability Act.

Strict regulation of chromates was anticipated by the chromium chemical supplier and user communities. Efforts have been underway for over 25 years to identify and develop replacement processes for chromate conversion. In spite of these efforts, widespread acceptance of replacement technologies has not occurred. This situation exists for several reasons. First, performance of new coatings do not yet equal those of chromate conversion coatings. This is particularly true for conversion coatings applied to aluminum alloys with high Cu or Si contents. Second, some of the new coatings are not applicable to a wide range of alloy substrates. Third, most of the new processes require multiple processing steps or application of heat (> 100° C) electrical potential, or current. This forces changes in plant processing equipment or process time that can not be easily accommodated on an industrial scale. Fourth, new coatings do not yet have a record of performance in service.

This paper describes the fundamental aspects of several related conversion coating methods that are potentially simple and low-cost. These methods are based on film formation that occurs when aluminum alloys are exposed to alkaline lithium salt solutions. These methods have the potential to be procedurally similar to traditional chromate conversion processes without the toxic hazard. The basic principles of film formation and general methods used to form the coatings are given. The resulting coating morphology, structure and composition are described. Finally, the corrosion resistance determined by electrochemical testing in aggressive chloride solutions is presented.

THE BASIC COATING FORMATION PROCESS

The basis of inhibited alkaline solution conversion coating is the reaction of aluminum with water at elevated temperatures (25° to 100° C). Experimental studies indicate that there are three primary steps in the reaction process which results in film growth on aluminum[4,5]. These are the formation of an amorphous oxide, dissolution of this oxide to a soluble aluminum species, and precipitation of these species as a hydrous oxide. At temperatures less than boiling and with sufficient time, the reaction process results in a duplex film with a poorly crystalline boehmite (AlOOH) or pseudoboehmite inner layer and a crystallized bayerite ($Al(OH)_3$) outer layer. This particular film structure is obtained due to the formation kinetics of the phases involved in the process: amorphous pseudoboehmite forms rapidly but does not readily crystallize; dissolution of this compound liberates sufficient aluminum ion to enable precipitation of crystalline boehmite, and at longer times bayerite forms.

In alkaline solutions, aluminum oxides are very soluble and the film dissolution-precipitation process proceeds rapidly and for long times before the aluminate ion concentration in solution attains the solubility limit which enables precipitation. As a result, the metal substrate experiences severe etching and corrosion. Additionally, the film that finally forms is more porous, hence less corrosion resistant

than one that forms at lower pH. The presence of lithium in alkaline solutions does not appear to alter the basic aluminum-water reaction sequence but it does alter the phases formed, increases the kinetics of film formation to suppress unwanted etching, and results in formation of a more corrosion resistant film.

Figure 1 is a scanning-transmission electron micrograph of the duplex film formed on aluminum during a 15 minute exposure to a mixed lithium carbonate-sodium aluminate solution at pH 11.5. This two layer film is structurally similar to that described above. However, the film is quite thick for the small reaction times used, and the phases formed are different than those normally formed by the reaction of aluminum with water. Figure 2 shows a grazing incidence angle X-ray diffraction pattern for the surface coating shown in Figure 1. This pattern indicates the presence of $Li_2[Al_2(OH)_6]_2{\cdot}CO_3{\cdot}3H_2O$ which belongs to the hydrotalcite mineral family[6]. Electron diffraction of the inner layer indicates poor crystallinity similar to observations for hydrous aluminum oxide films[7]. Secondary ion mass spectroscopy of films formed on commercially pure aluminum under similar conditions indicates that this inner layer contains lithium and is therefore compositionally different than conventional hydrous aluminum oxide films. It has not been determined if this compositional difference results in a change in transport properties of this layer.

In alkaline solutions, hydrotalcite is less soluble than bayerite which may contribute to the increased film formation rate. Figure 3 is a plot of bayerite and hydrotalcite solubility as a function of solution pH[7]. Between pH 10 and 13, hydrotalcite is less soluble than bayerite and would therefore be expected to form preferentially. The notion that hydrotalcite is formed in preference to bayerite is substantiated by X-ray diffraction studies that indicate that the predominant compound formed under these conditions is hydrotalcite.

Among Group IA and IIA cation salts only lithium salts appear to be suitable for use in coating formation for practical purposes. Additions of lithium, magnesium and calcium salts to alkaline solutions have been observed to promote film formation and passivation of aluminum alloys [8-17]. Magnesium, calcium and strontium are potent hydrotalcite formers but their solubility in alkaline solutions is low and hydrotalcite formation is sluggish. Sodium, potassium, rubidium and cesium salts are all highly soluble in alkaline solutions, but none form hydrotalcites. As the lowest atomic number element in its group (neglecting hydrogen), lithium shares chemical properties of both Group IA and Group IIA. Therefore only lithium salts exhibit requisite solubility and capacity for hydrotalcite formation that enable passive film formation in short periods of time. The salt anion appears to be less critical in determining passive film formation. Passivating hydrotalcite films have been formed from alkaline lithium salt solutions including lithium hydroxide, sulfate, bromide, chloride and borate.

Aluminum ion, speciated as aluminate AlO_2^-, or equivalently $Al(OH)_4^-$, is also critical to formation of passivating hydrotalcite films. Figure 4 shows the open circuit potential (OCP) of 99.999 Al in a 7.4 g/L Li_2CO_3 plus 200 ppm AlO_2^- solution at pH 11.5 as a function of time. During this exposure the potential shifts in the positive direction by more than 1.0 V due to passive film formation. To demonstrate the role of aluminum in the film formation process, anodic polarization curves were collected before and after passivation was complete. Figure 5 shows an anodic polarization curve collected after 650 seconds of OCP exposure. At this point, the surface is incompletely passivated and the aluminum sample experiences an active to passive transition as sufficient aluminate ion is generated by dissolution to enable film formation. The contrasting situation is shown by the polarization curve collected after 52000 seconds of OCP exposure. In this case, the Al surface exhibits passive behavior only. Passivity is observed because sufficient aluminate ion was generated by dissolution under OCP conditions over the long exposure duration to enable complete film formation.

Based on these types of experiments, the requisite ingredients for hydrotalcite film formation on a short time scale are: a lithium salt, an aluminum salt (or an equivalent source for aluminate)and an alkaline pH. Coating formation will occur at ambient temperatures, but elevating the solution temperature promotes rapid film formation. Coatings with desirable properties can be formed on Al, Al-Mg, and Al-Mg-Si alloys by exposure to alkaline lithium-aluminum salt solutions for times as short as 5 minutes.

A MODIFIED PROCESS FOR ALUMINUM ALLOYS CONTAINING COPPER

In many aqueous surface finishing procedures including degreasing, deoxidizing and conversion coating, the presence of copper in the alloy substrate is problematic. During these processes, the surfaces of work pieces become enriched with a variety of copper compounds, occasionally including metallic Cu, that are collectively referred to as "smut". Cu smut forms in etching alkaline degreasing solutions where Cu solubility is low[18]. Less frequently, it is observed to accumulate on surfaces during deoxidation where aggressive chemical action intended to remove surface oxides attacks the underlying alloy substrate[7]. Metallic copper deposits form because the open circuit potential for the alloy substrate is negative to the reduction potential for Cu. Cu smut interferes with conversion coating formation[19], anodization[20] and with bonding of subsequently applied adhesives and paints[19,21,22]. It is also suspected to contribute to increased susceptibility to corrosion during service due to galvanic coupling with Cu-rich surface regions.

A possible remedy to this situation has been identified for conversion coating processes using alkaline Li salt solutions. A modification to the basic process enables simultaneous coating formation and Cu removal. This process modification is based on the fact that it is thermodynamically possible to use complexing reactions to extract and retain Cu in aqueous solution, and that Cu solubility increases appreciably in very alkaline solutions. Coatings formed using the modified coating process offer good corrosion resistance on 2024-T3 (Al-4.4Cu-2.5Mg-0.6Mn) in both electrochemical and exposure corrosion testing (salt spray).

High corrosion resistance is due in part to removal of Cu compounds from the coating. The removal of Cu from the surface film can be explained by copper solubility in alkaline solutions and by copper complex formation by carbonate. The solubility minimum for Cu occurs at pH 9.8. At pH 11.5, the pH of the first stage coating bath, Cu solubility is less than 10^{-8} M. Cu enrichment in the surface film during exposure to this solution is therefore expected. At pH 13.5, Cu solubility increases to approximately 5×10^{-4} M. Since hydrotalcite formation is still possible at this pH, a Cu-free film forms. Removal of Cu is assisted by Cu complex formation which further increases the total solubility for Cu^{2+}. At pH 13.5 the following complex formation process is possible:

$$Cu^{2+} + 2CO_3^{2-} \rightarrow Cu(CO_3)_2^{2-}\ (aq) \qquad \text{(eq. 1)}$$

$$K_{form} = 9.83 \pm 0.04.$$

To illustrate how this modification to the process works, it is helpful to compare it to the more mature variant that offers good corrosion resistance on Al, Al-Mg and Al-Mg-Si alloys, but does not perform well on Al-Cu-Mg alloys. This process, which will be referred to as the "basic" process, is formed in a solution containing 7.4 g/L Li_2CO_3 plus 200 to 400 ppm $Na_2Al_2O_4$ with a pH of 11.2 to 11.8 at 50±5° C for 15 minutes. In the modified process, the basic process is carried out followed immediately by a second immersion step carried out in a solution containing 7.4 g/L Li_2CO_3, 7.2 g/L LiOH and 11.1 g/L $Na_2Al_2O_4$ with a pH of 13.5. This solution is also operated at a temperature of 50±5° C and immersion times range from 15 to 180 minutes. The modified process has been used to generate highly corrosion resistant coatings on 2024-T3.

Figure 6 is a scanning electron micrograph (SEM) of a surface of a 2024-T3 sample after hydrotalcite coating with the basic process. The surface is featureless except for cracks that formed by shrinkage as the film dried. Figure 7 shows the surface morphology after coating according to the modified process. In this case, the distinctive surface morphology associated with hydrotalcite coatings is observed[23]. Grazing incidence angle x-ray diffraction of the coating formed by the basic process shows that the primary compound in the coating is bayerite, $Al(OH)_3$. However, coating formed using the modified process contains hydrotalcite with no detectable amounts of bayerite.

Figures 8 and 9 show oxygen, copper and aluminum sputter depth profiles determined by auger electron spectroscopy (AES) for the surface of 2024-T3 coated using the basic and modified processes respectively. The surface film and substrate regions can be clearly distinguished by the sharp decrease in the oxygen signal and the corresponding increase in the Al signal after 3500 seconds of sputtering time. In Figure 8, the Cu profile exhibits a broad maximum with a peak concentration that is approximately 4 times the concentration present in the alloy substrate. In Figure 9, the profile shows that use of the modified process results in no enrichment of the coating above levels that are present in the alloy substrate. As in Figure 8, the oxide-metal interface is reached after approximately 2000 seconds of sputtering time indicating no net change in film thickness assuming similar sputter rates for each film.

METAL OXIDE MODIFIED COATINGS

A third process variant has been identified for less corrosion resistant substrates including 2024-T3 and 7075-T6. This process involves deposition of a hydrotalcite coating followed by exposure to an aqueous neutral or acid metal salt solution. This second step is intended to seal any latent porosity by precipitating metal oxide into pore spaces. This process is analogous to dichromate sealing of sulfuric acid anodized aluminum except that external electrolytic control is not required and the second sealing step can be completed in a very short period of time. The corrosion resistance of a sealed hydrotalcite coating is not as effective as that of a sealed anodized coating, but it is good compared to chromate conversion coatings.

The metal salts used in the second step of this coating process can be divided into two sets. The first set consists of salts whose solubility minimum occurs under alkaline solution conditions. This includes salts of Ce, Co, Ni, Fe, Mn and Mg. The second set consists of metals, not included in the first class, but considered as potential inorganic sealants for oxide coatings. This includes salts of Mo, Bi, Al and Cr (Cr salts were used for reference only).

In these processes, hydrotalcite coatings are formed using one or the other of the two processes described in the earlier sections. The workpieces are then immediately immersed in the metal salt solution for a period of time ranging from seconds to tens of minutes.

During exposure to a transition metal salt solutions, the coating morphology, structure and composition of the original hydrotalcite coating change. The case of sealing with Ni-acetate (Ni-Ac) is given as a representative example. Figures 10 and 11 are scanning electron micrographs of a hydrotalcite coated 6061-T6 surface before and after 5 and 30 minutes exposure to a pH 6.5 Ni acetate solution respectively. The distinct hydrotalcite coating morphology is retained after 5 minutes exposure but not after the 30 minutes exposure. Grazing incidence angle X-ray diffraction (GIXRD) detected the major reflections for the hydrotalcite compound in the coating formed by the 30 minute exposure, but some of the minor peaks are absent. Peaks due to formation of other compounds including $Ni(OH)_2$ were not detected. This suggests degradation of the hydrotalcite compound with possible replacement by an amorphous hydroxide compound during extended exposure. Figures 12 and 13 show sputter depth profiles of a hydrotalcite surface exposed to Ni-Ac solution for 5 and 30 minutes. After 5 minutes, Ni is detected in the outer portion of the coating. As exposure time increases the total coating thickness increases and the total amount of Ni in the coating increases. These data suggest degradation or replacement of hydrotalcite with a Ni-based compound after long exposures to the Ni-Ac solution.

COMPARISON OF COATING CORROSION RESISTANCE

Corrosion resistance was evaluated using electrochemical impedance spectroscopy (EIS). EIS spectra were collected from conversion coated samples after 24 hours exposure to a 0.5 M NaCl solution. The total exposed area of coated surface to solution was 16 cm^2. Data were collected from 10 kHz to 10 mHz using a 10 mV sinusoidal voltage perturbation. A minimum sampling rate of 7 points

per decade frequency was used. Spectra for these samples usually exhibited a capacitive, though slightly lossy response from 1 kHz to 100 mHz. In some cases, at the lowest measured frequencies a DC limit or transmission line response was detected indicating corrosion by pitting. A representative Bode impedance magnitude plot for 2024-T3 coated using each of the three processing variants described is shown in Figure 14.

EIS spectra were analyzed by equivalent circuit modeling. Spectra were fit to a model using complex non-linear least square (CNLS) method[24]. The models used for fitting were derived from the model proposed by Hitzig et. al. for the EIS response for aluminum covered by a damaged oxide film[25]. In some cases distributed elements were substituted for the discrete elements in Hitzig's model, and whenever possible, simplified versions of the model were used to fit data. Most of the spectra were fit using the simplified model shown in Figure 15. This model consists of a solution resistance in series with a parallel resistor-constant phase element (CPE) combination. The use of a CPE rather than a discrete capacitor enables fitting of these inherently lossy coatings. The admittance of the CPE is given by:

$$Y(\omega) = (j\omega\tau)^{\phi} \qquad \text{(eq. 2)}$$

where j is $\sqrt{-1}$, ω is the frequencies in radians, τ is a time constant, and ϕ is an exponent whose value ranges from 0 to 1. The primary figure of merit derived from equivalent circuit modeling is the magnitude of the resistance due to the corrosion process, R_{cor}. For highly corrosion resistant chromate conversion coatings, an R_{cor} value of 1 to 2 $M\Omega \cdot cm^2$ can be expected for the exposure regimen used here. This value can be used as a benchmark in evaluating the corrosion performance data for coated samples shown in Figures 16 and 17.

Figure 16 shows R_{cor} values for coatings applied to 6061-T6. This plot summarizes data from each of the three types of processes described and plots R_{cor} versus cumulative process time (excluding degreasing and deoxidation). Groups of data occur at certain discreet process times. The range in the R_{cor} values in a given group represent coatings prepared using different processes (e.g. different sealing baths operated for the same length of time) and do not represent scatter for a single process. Assignment of individual coating processes to individual data points will be made at a later time. The closed symbols indicate R_{cor} values for the basic process and the open symbols indicate R_{cor} values for the modified processes. The solid lines bound the majority of the data set. the data in this plot suggest that the metal oxide modification to the basic coating process can produce useful gains in corrosion resistance without adding a large amount of time to the coating process. For example, using a 5 minute transition metal sealing step after depositing a hydrotalcite coating can increase R_{cor} by an order of magnitude. Sealing a hydrotalcite coating for times longer than 5 minutes does not appear to provide much additional corrosion resistance. In some cases corrosion resistance is worse that for the basic process.

Figure 17 shows an R_{cor} versus process time plot for coated 2024-T3. This plot was constructed in a manner identical to that for Figure 16. Again the R_{cor} values for the basic process are shown by the closed symbols and R_{cor} for the modified processes are shown with open symbols. Two items are immediately obvious in comparison with the 6061-T6 data. First, for any given process time, R_{cor} for 2024-T3 is less than that for 6061-T6. This is probably a reflection of the low intrinsic corrosion resistance of Al-Cu-Mg alloys. Second, R_{cor} values improve continuously with increased process time. This somewhat unfortunate response indicates that using current methods, high corrosion resistance can not be attained in less than 80 minutes of process time. However, past experimentation with these processing methods has generally resulted in identification of means for improving corrosion resistance and decreasing total process time. To date, no information has been collected that suggests a change in these trends.

Empirical evidence collected from tests conducted in our laboratories and others[26] suggests that for 6061-T6 when an R_{cor} value greater than 10^5 ohm-cm^2 is measured a coated sample can be expected to withstand 168 hours of salt spray exposure testing without pitting. For 2024-T3 an R_{cor} value greater

than 10^6 ohm-cm^2 usually indicates that a coated sample will perform well in salt spray exposure. The data in Figure 16 show that coatings formed using the basic process can be expected to perform well in salt spray exposure testing. This has been observed to be the case[27]. Using the metal oxide modified process, which adds 5 minutes of processing time, coatings can be formed that almost always exceed the 10^5 ohm-cm^2 threshold. Performance of these coatings in salt spray exposure testing is uniformly good suggesting that the metal oxide modification is the process of choice for high corrosion resistance. Forming a coating on 2024-T3 with good corrosion resistance requires considerably more processing time. The data from this study indicate a minimum of 80 minutes to achieve the 10^6 ohm-cm^2 R_{cor} threshold. Panels produced using these methods demonstrate significantly improved corrosion resistance over those formed using the basic process. However, unacceptable amounts of pitting are sometimes observed after 168 hours of salt spray exposure. The current situation is that uniformly acceptable salt spray performance is only observed for coatings formed using the longest coating processes. In this case, further process development is required to shorten process time and increase corrosion performance.

SUMMARY

Exposure of aluminum alloys to alkaline lithium salt solutions containing aluminate results in formation of a duplex surface film whose primary component is a hydrotalcite compound. This film is continuous across the surface and provides good corrosion resistance for Al, Al-Mg and Al-Mg-Si alloy substrates. To form corrosion resistant coatings on less corrosion resistant substrates like Al-Cu-Mg alloys, modifications to the basic process must be made. A modified process has been devised that can extract Cu compounds from the coating that may degrade its protective capacity. This process exploits Cu solubility at high pH and Cu complexing to produce Cu-free coatings. Corrosion resistant coatings can also be made by reinforcing a hydrotalcite coating with other metal oxides. These oxides are deposited in or on the coating using a second processing step. Each of these process variants improves the corrosion resistance over the basic process while retaining the simplicity and procedural similarity to traditional conversion coating operations.

ACKNOWLEDGMENTS

The author wishes to thank M. Martinez sample preparation and electrochemical corrosion testing. W. Buttry and B. McKenzie for surface analysis and scanning electron microscopy.

REFERENCES

1.) J. Spruance, American Chemical Paint Co., U.S. Patent 2 438 887 (1948).

2.) Chemical Marketing Rep., 238, 1, p. 222 (1990).

3.) The Aluminum Industry WWW Server, http://www.euro.net:80/concepts/industry.html, Integrated Concepts, Inc. WWW Development, European Multimedia Engineering, B.V., Oud Beijerland, Netherlands (1995).

4.) W. Vedder, D.A. Vermilyea, Trans. Faraday Soc., 65, p. 561 (1969).

5.) R.S. Alwitt, J. Electrochem. Soc., 121, p. 1322 (1974).

6.) C.J. Serna, J.L. Rendon, J.E. Iglesias, Clays and Clay Minerals, 30, p. 180 (1982).

7.) C.A. Drewien, R.G. Buchheit, "Issues for Conversion Coating of Aluminum Alloys with Hydrotalcite", CORROSION/94. paper no. 622 (Houston, TX: NACE International, 1994).

8.) R. B. Mears, L. J. Benson, Ind. & Eng. Chem., 32, p. 1343 (1940).

9.) M. Mushiro, K. Shigoka, Met. Fin. Jpn., 23, p. 370 (1972).

10.) T. Uchiyama, T. Abe, Jpn Inst. Light Met.32, p. 202 (1982).

11.) V.V. Sysoeva, E.D. Artyugina, V.G. Gorodilova E.A. Berkman, Z. Prikladnoi Khim., 58, p. 921 (1985).

12.) T. Uchiyama, M. Hasegawa, H. Matsumoto, Met. Fin. Jpn., 37, p. 178 (1986).

13.) J. Gui, T.M. Devine, Scripta Met., 21, p. 853 (1987)

14.) J. Craig, R.C. Newman, M.R. Jarrett, N.J.H. Holroyd, J. Phys., 48, p. 825 (1987).

15.) Y. Isobe, S. Tanaka, M. Masaki, F. Hine, Boshoku Gijutsu, 38, p. 161 (1989).

16.) S. Tanaka, Y. Isobe, F. Hine, Boshoku Gijutsu, 39, p. 425 (1990).

17.) C.M. Rangel, M.A. Travassos, Corros. Sci., 33, p. 327 (1992).

18.) M. Pourbaix, *Atlas of Electrochemical Equilibria in Aqueous Solutions*, p. 389 (Houston, TX, NACE, 1974).

19.) N. Fin, H. Dodink, A.E. Yaniv, L. Drori, *Applied Surface Science*, **28**, p. 11 (1987).

20.) J.S. Solomon, N.T. McDevitt, *Thin Solid Films*, **84**, p. 155 (1981).

21.) A.V. Pocius, T.H. Wilson, Jr., S.H. Lundquist, S. Sugii, in *Progress in Advanced Materials and Processes: Durability, Reliability and Quality Control*, G. Bartelds, R.J. Schekelmann, Eds., p. 71 (Amsterdam: Elsevier Science Publishers B.V., 1985).

22.) T.S. Sun, J.M. Chen, J.D. Venables, *Applications of Surface Science*, **1**, p. 202 (1978).

23.) R.G. Buchheit, M.D. Bode. G.E. Stoner, *Corrosion*, **50**, p. 205 (1994).

24.) ZSIM for Windows, Scribner and Associates, Charlottesville, VA.

25.) J. Hitzig, K. Juttner, W.J. Lorenz, J. Electrochem. Soc., 133, p. 897 (1986).

26. M.W. Kendig, private communication, 1995.

27.) R.G. Buchheit, C.A. Drewien, J.L. Finch, G.E. Stoner, "Non-Chromate Conversion Coatings for Aluminum", CORROSION/94, paper no. 542, (Houston, TX:NACE International, 1994).

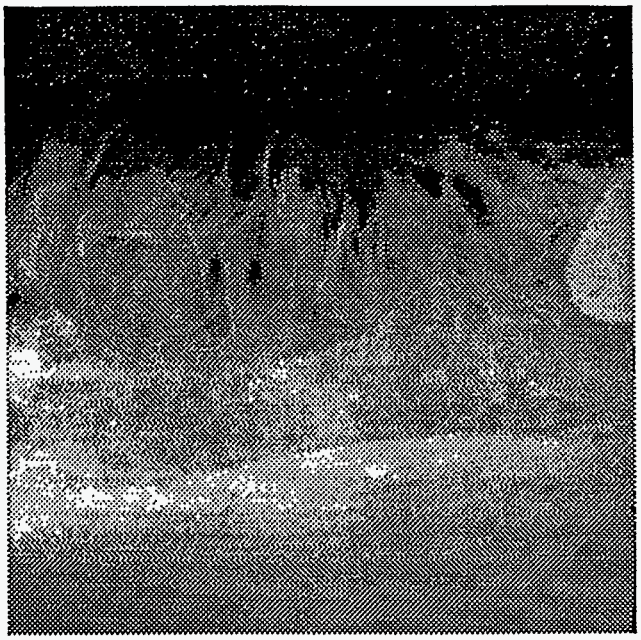

Figure 1. Scanning transmission electron micrograph of the duplex film formed by reaction of aluminum with an alkaline lithium aluminum salt solution.

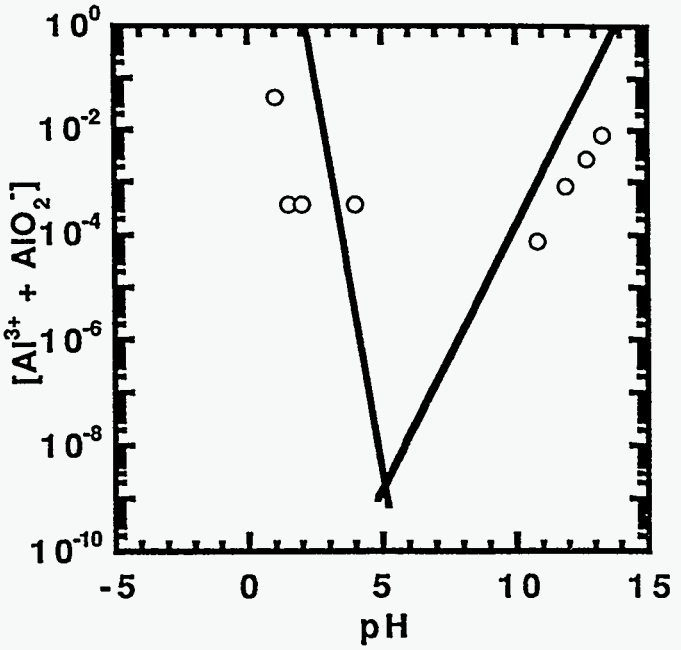

Figure 3. Bayerite and hydrotalcite solubility plotted as a function of solution pH. Bayerite is indicated by the solid lines, hydrotalcite by the data points.

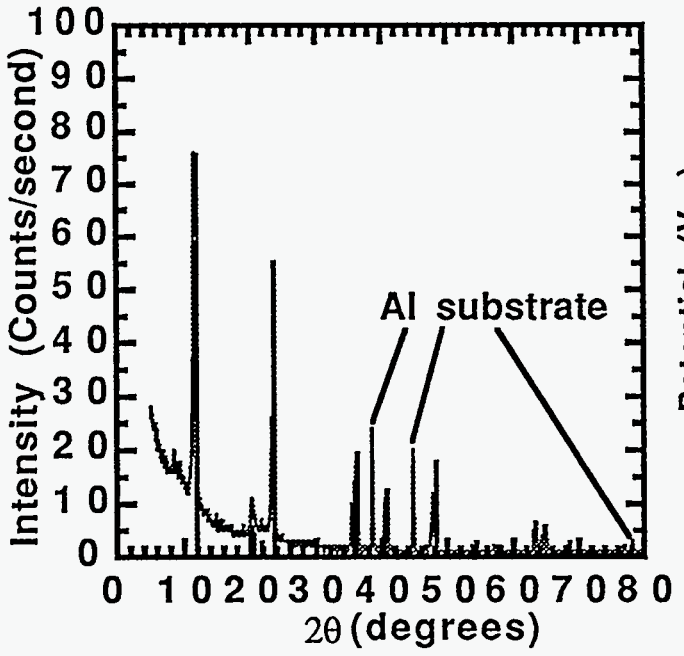

Figure 2. GIXRD pattern from the coated Al surface shown in Figure 1. The dominant compound identified is hydrotalcite. Vertical lines indicate the reference pattern.

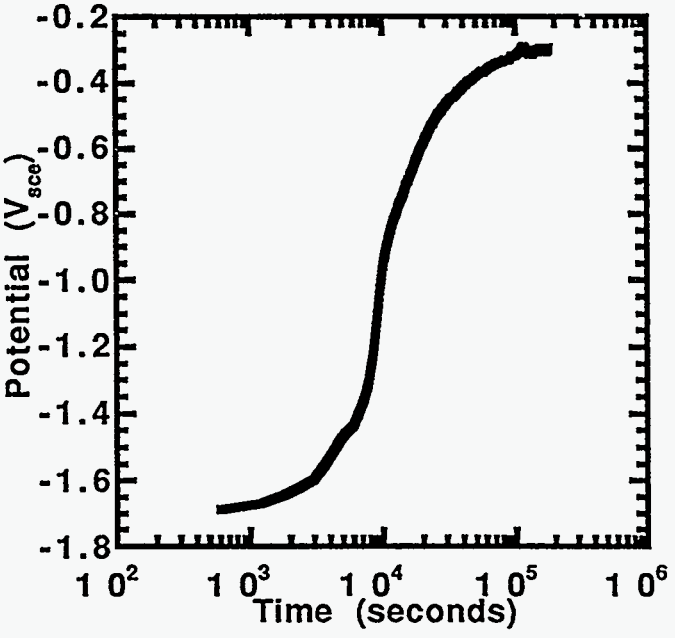

Figure 4. Open circuit potential of 99.999Al in 7.4 g/L Li_2CO_3 plus 200 ppm AlO_2^- pH 11.5 as a function of time.

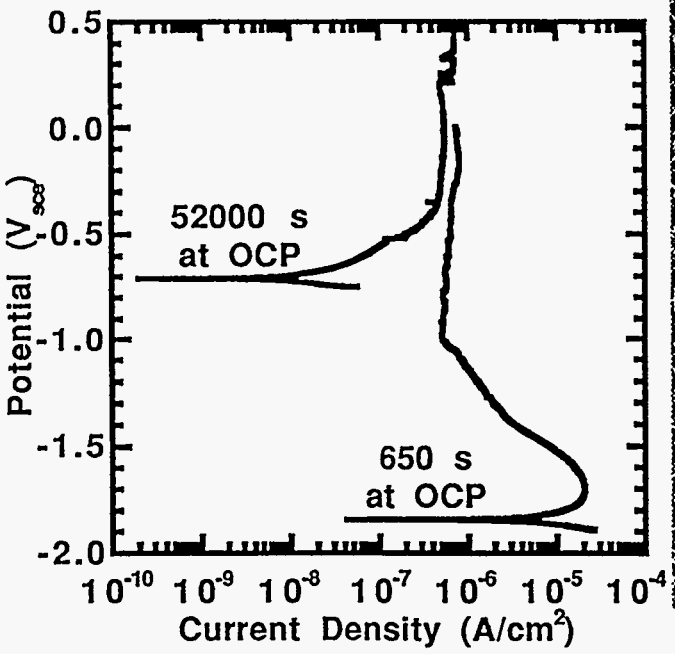

Figure 5. Anodic polarization curves for 99.999 Al in 7.4 g/L Li_2CO_3 plus 200 ppm AlO_2^- after different lengths of exposure time at OCP.

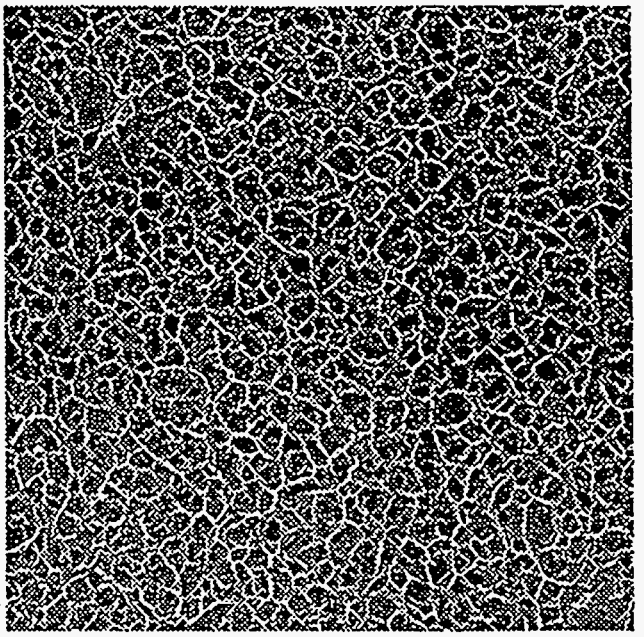

10 μm

Figure 7. Scanning electron micrograph of the coating formed on 2024-T3 using the modified coating process.

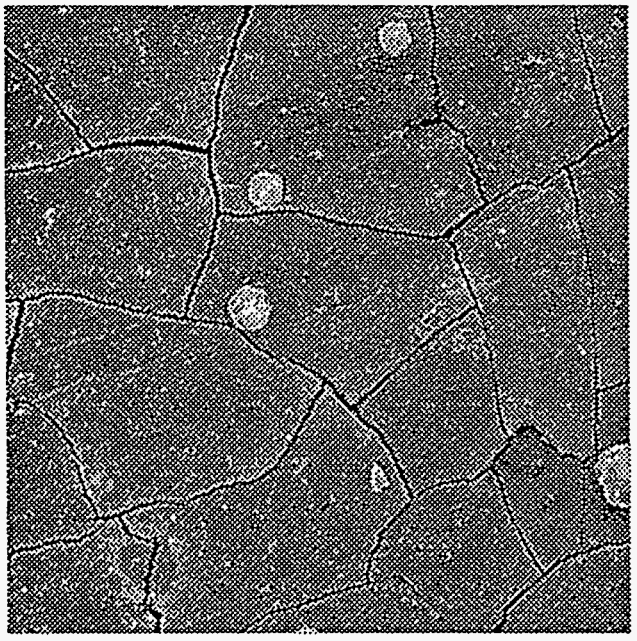

10 μm

Figure 6. Scanning electron micrograph of the coating formed on 2024-T3 using the control coating process.

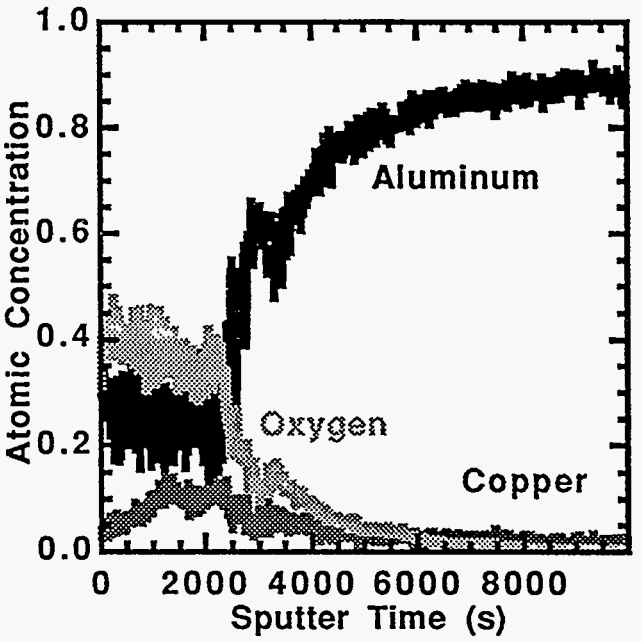

Figure 8. Auger electron spectroscopy sputter depth profiles for Al, Cu and O on 2024-T3 coated using the control process.

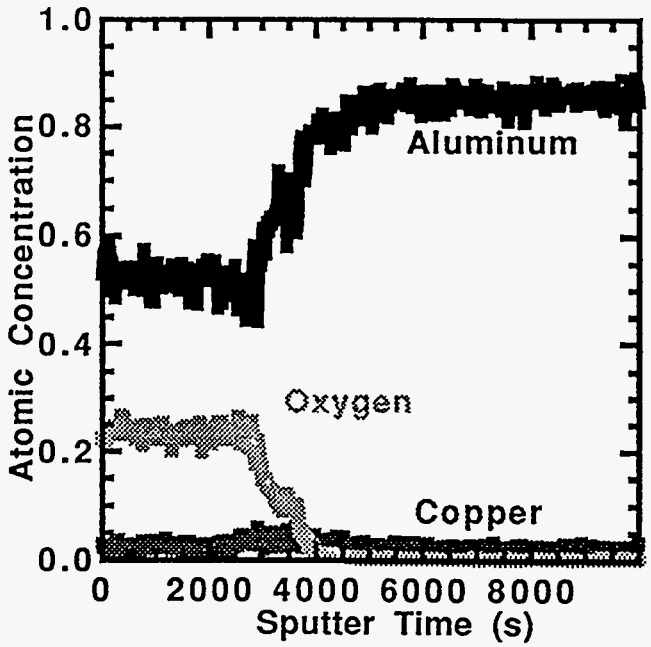

Figure 9. Auger electron spectroscopy sputter depth profiles for Al, Cu and O on 2024-T3 coated using the modified process.

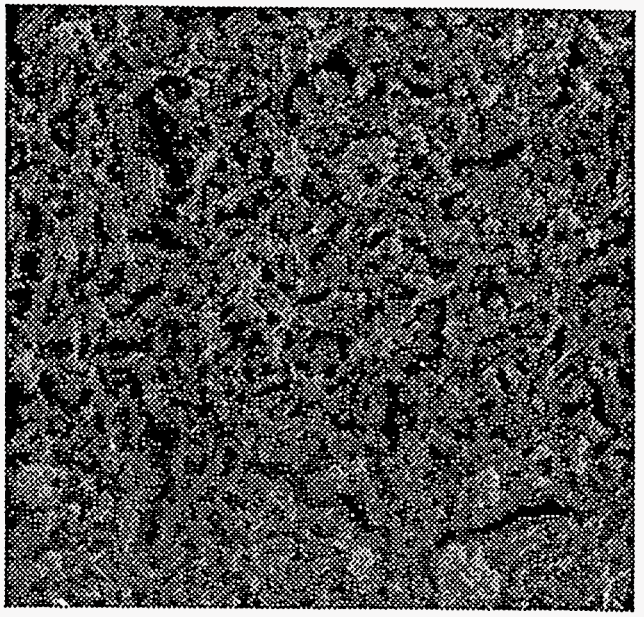

Figure 11. Scanning electron micrograph of a hydrotalcite coated 6061-T6 surface after exposure to a Ni-Ac solution for 30 minutes.

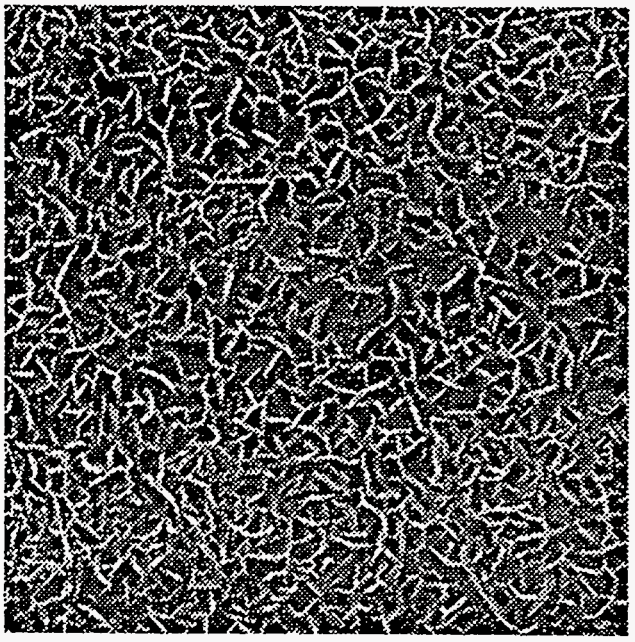

Figure 10. Scanning electron micrograph of a hydrotalcite coated 6061-T6 surface after exposure to a Ni-Ac solution for 5 minutes.

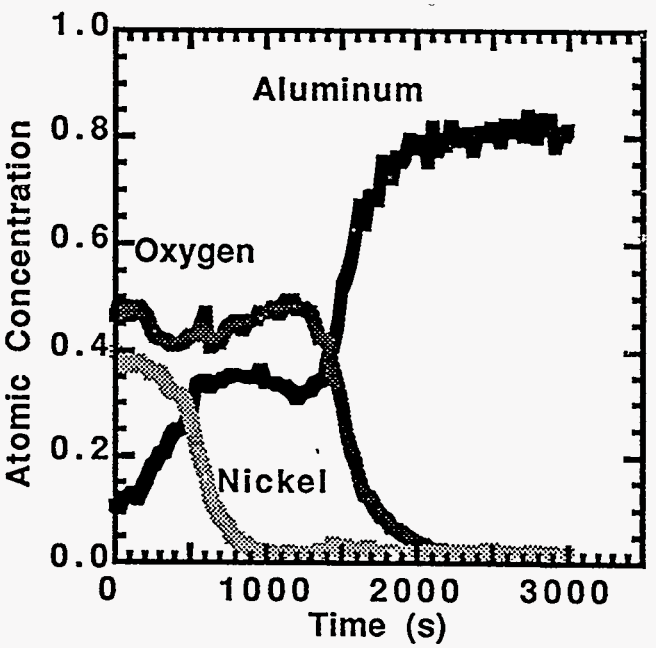

Figure 12. Auger electron spectroscopy sputter depth profiles for Al, O and Ni on 6061-T6 coated and exposed to a Ni-Ac solution for 5 minutes.

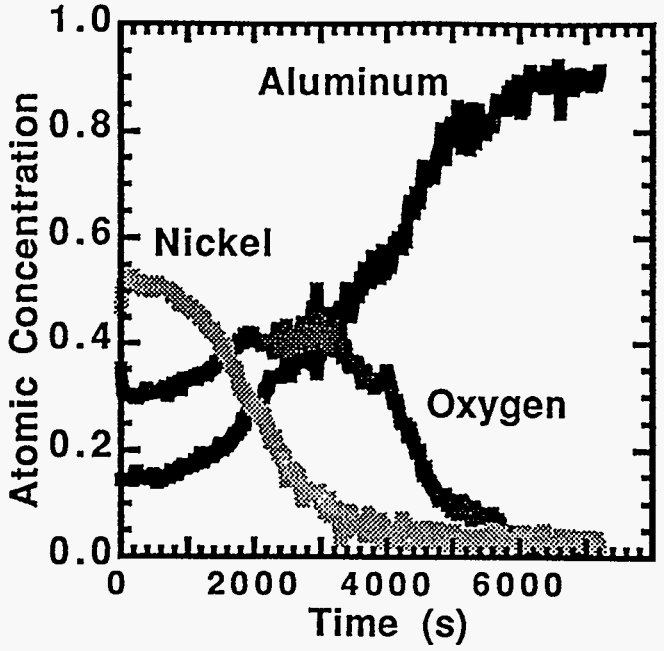

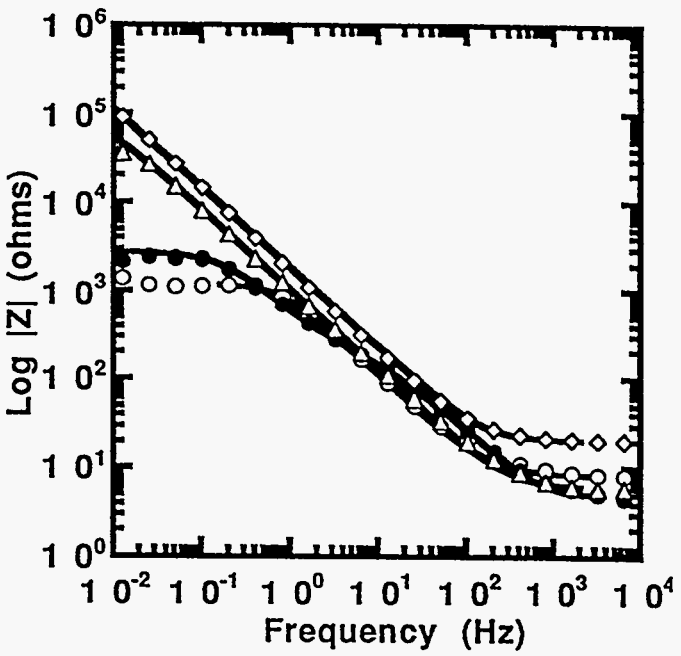

Figure 13. Auger electron spectroscopy sputter depth profiles for Al, O and Ni on 6061-T6 coated and exposed to a Ni-Ac solution for 30 minutes.

Figure 14. Bode impedance magnitude plots for bare 2024-T3 (o), coated using the original process (•), coated using the modified process (Δ), and coated using the Ce oxide modified process (◊). The symbols represent EIS data and the solid line represent the CNLS fit.

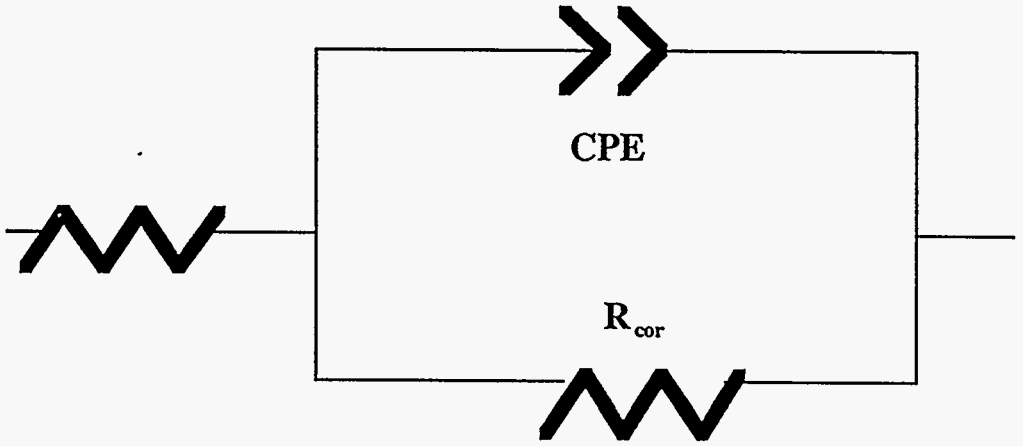

Figure 15. Schematic illustration of the equivalent circuit model used to fit most of the EIS data.

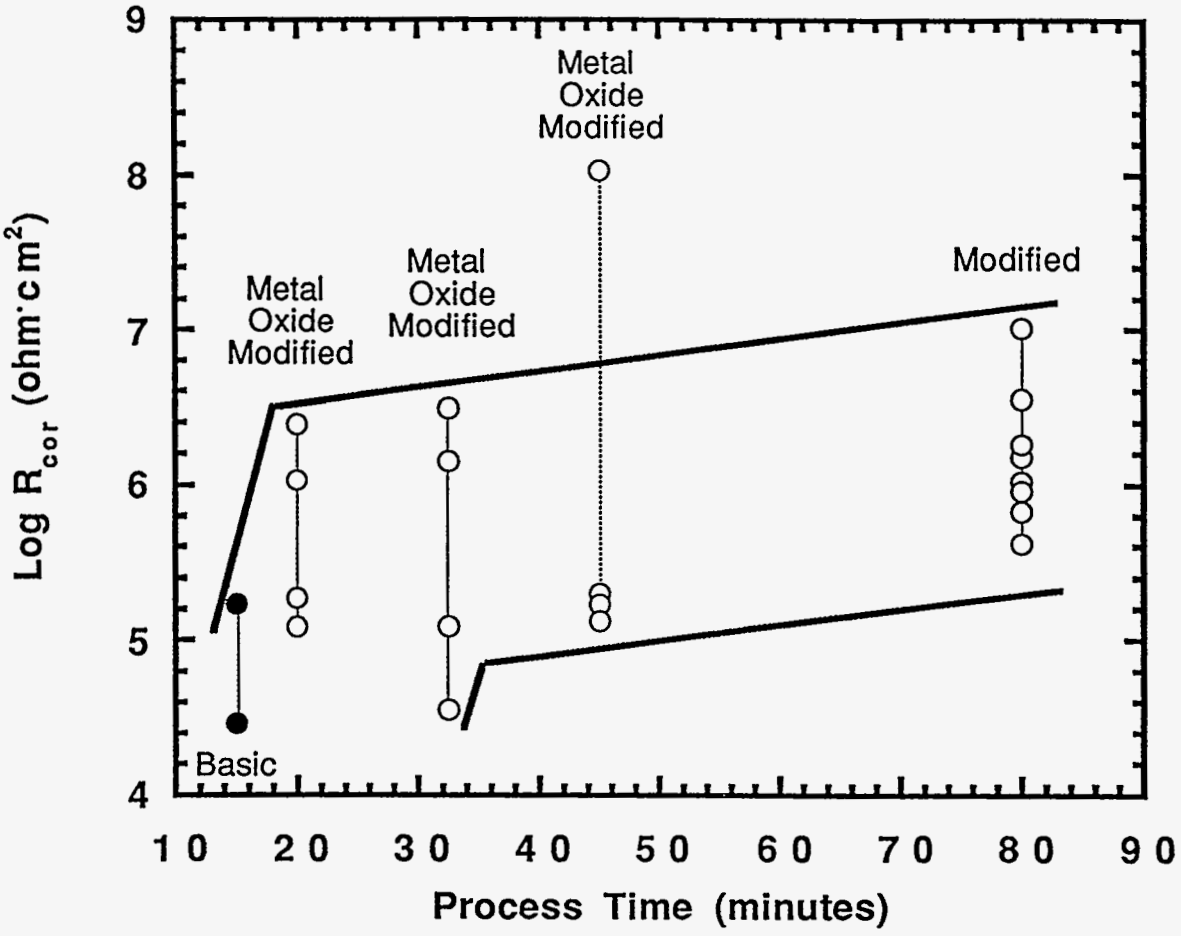

Figure 16. R_{cor} versus total process time for coated 6061-T6. The vertical lines indicate Rcor data from related, though not identical, coating processes.

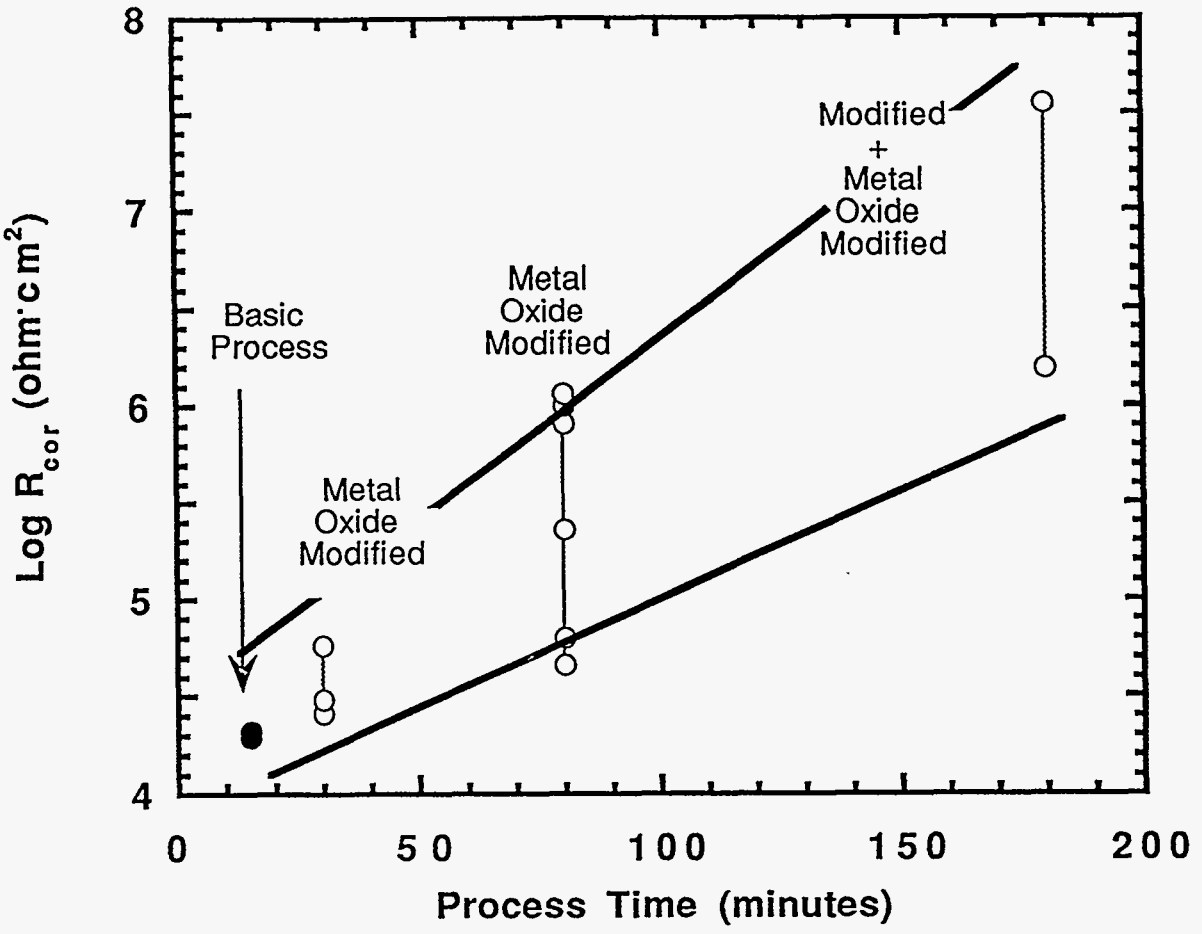

Figure 17. R_{cor} versus total process time for coated 2024-T3. The vertical lines indicate Rcor data from related, though not identical, coating processes.